STUDIA UBB PHYSICA, Vol. 60 (LX), 1, 2015, pp. 61-72
(RECOMMENDED CITATION)

Dedicated to Academician Professor Dr. Emil Burzo on His 80th Anniversary

MODELING OF CRYSTAL FIELD PARAMETERS AND ENERGY LEVELS SCHEME SIMULATION FOR Fe^{6+} DOPED IN K_2MO_4 (M= Cr, S, Se)

M.G. BRIK[1,2,3,4], E.-L. ANDREICI[5] AND N.M. AVRAM[5,6*]

ABSTRACT. In this paper we report the results of a detailed comparative crystal field analysis of the crystal field parameters and energy level schemes, for all three above mentioned materials. The crystal structure data was used to calculate the crystal field parameters in the framework of exchange charge model using the Symmetry Adapted Axis System centered at the impurity ion. A thorough consideration of the impurity center symmetry was performed and the calculated crystal field parameters were used to diagonalize the crystal field Hamiltonian for each system. Energy levels obtained in this way were compared with the corresponding experimental data to yield good agreement between the theoretical and experimental results.

Keywords: *Fe^{6+}, K_2SO_4, K_2CrO_4, K_2SeO_4, crystal field parameters, energy levels.*

INTRODUCTION

Crystals doped with transition metal ions V^{3+}, Cr^{4+}, Mn^{5+}, Fe^{6+} (all of them have the $3d^2$ electron configuration) were, over the last years, the subject of systematic studies because of their potential applications as solid-state laser active media and electro optical devices [1, 2]. After doping, these ions usually occupy the sites with tetrahedral coordination, which can be described in terms of either low (V^{3+}, Cr^{4+}) or

[1] *College of Sciences, Chongqing University of Posts and Telecommunications, Chongqing 400065, P.R. China*
[2] *Institute of Physics, University of Tartu, Ravila 14C, Tartu 50411, Estonia*
[3] *Institute of Physics, Polish Academy of Sciences, Al. Lotnikow 32/46,Warsaw 02-668, Poland*
[4] *Institute of Physics, Jan Dlugosz University, Armii Krajowej 13/15, PL-42200 Czestochowa, Poland*
[5] *Department of Physics, West University of Timisoara, Bd. V. Parvan, No. 4, 300223, Timisoara, Romania*
[6] *Academy of Romanian Scientists, Independentei 54, 050094-Bucharest, Romania*
** Corresponding author e-mail: avram@physics.uvt.ro*

strong (Mn^{5+}, Fe^{6+}) crystal field [2]. Speaking about the ferrate (VI) ion, it is worth noting that it is perfectly stabilized in well-defined tetrahedral oxo coordination. Experimentally the absorption and luminescence spectra of Fe^{6+} ion in the K_2MO_4 (*M*= Cr, S, Se) crystals have been investigated [1, 3-5], including the Fe^{6+} excited states properties [4]. Wagner *et al* [6] studied the EPR spectra of the single crystals and powders with an aim of getting a better insight into the properties of the Fe-O bond and the site geometry of the FeO_4 polyhedral in various hosts. The density functional theory (DFT)-based study of the optical excitations and coupling constants in FeO_4 ion was reported in Ref. [7], and *ab initio* study of the absorption properties of the same complex can be found in Ref. [8].

However, until now no satisfactory and unified theoretical description and explanation for optical spectral data regarding title systems, in the framework of the crystal field theory wasn't offered. Previously, both experimental [1,4,5] and theoretical [7,8] papers have not used the actual C_s site symmetry of the Fe^{6+} centers, but the C_{3v} and T_d site symmetries, respectively. Therefore, in this paper we try to fill in this gap by reporting a detailed analysis of crystal field effects, modeling of the crystal field parameters (CFPs) and simulations of the energy level schemes for Fe^{6+} ion in three crystals K_2CrO_4, K_2SO_4 and K_2SeO_4, respectively.

The CFPs were modeled in the framework of the exchange charge model (ECM) of crystal field (CF) [9], using the actual crystal structure data in the Symmetry Adapted Axis System (SAAS) [10]. Application of the ECM implies knowledge of the overlap integrals between the *d*-functions of central ion and *s*, *p* functions of the ligands, which were calculated numerically with the wave functions from Ref. [11]. With the obtained CFPs we calculated the Fe^{6+} energy levels by diagonalizing the CF Hamiltonians of considered doped systems. The obtained results are discussed; quite satisfactory agreement with the experimental data [1, 4] was obtained.

SYMMETRY OF CRYSTALS

At room temperature, $K_2(M)O_4$ (M= Cr, S, Se) crystallizes in the orthorombic D_{2h}^{16}(Z=4) space group (number 62 in International Tables for Crystallography [12]), with α=β=γ=90° and a=7.663 Å, b=10.388 Å, c=5.922 Å for M=Cr [13], a=5.7704 Å, b=10.0712 Å, c=7.4776 Å, for M=S [14] and a=7.66 Å, b=6.00 Å, c=10.47 Å for M=Se [15], respectively (see Fig. 1).

It is essential that the Fe^{6+} ions in all considered K_2MO_4 crystals isovalently substitutes the M^{6+} ions, so no need for the charge compensation. The $[FeO_4]^{2-}$ cluster has the C_s site symmetry at room temperature. Under 93 K the K_2SeO_4 crystal has ferroelectric phase, with space group $Pna2_1$ (C_{2v}^9, Z=12) - number 62 in International Tables for Crystallography [12]). In this phase the parameters of the unit cell are α=β=γ=90°, a=22.716 Å, b=10.339 Å, c=5.967 Å, with the C_1 actual site symmetry of Fe^{6+} doped in K_2SeO_4 [16].

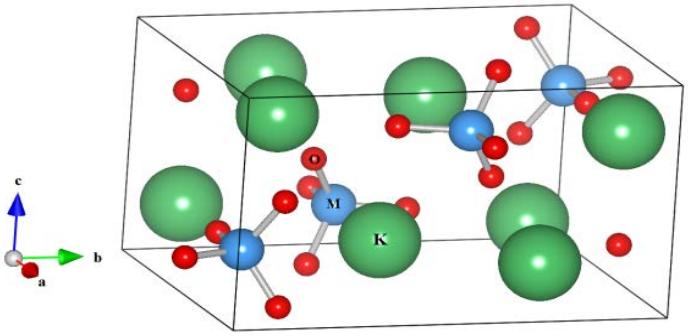

Fig. 1. One unit cell of K_2MO_4 (M= Cr, S, Se). The M ions are shown by the blue spheres tetrahedral coordinated by oxygen ions (red spheres) and K^+ ion are shown the by green spheres.

DESCRIPTION OF THE METHOD USE IN CALCULATIONS

In the present work for calculations of the CFPs we use ECM [9] of crystal field which is briefly described below.

In its framework the actual C_s (K_2CrO_4, K_2SO_4) respectively C_1 (K_2SeO_4) site symmetries of the ferrate (VI) ion, in three different host matrices, is considered. It is well known that in the frame of ECM, the crystal field Hamiltonian of the system will be written as [9]:

$$H = \sum_{p=2,4} \sum_{k=-p}^{p} B_p^k O_p^k \tag{1}$$

where O_p^k are the linear combinations of irreducible tensor operators acting on angular parts of the 3d-ion wave functions, and B_p^k are the CFPs containing all information about geometrical arrangement of the ligands around the central ion. Following Ref. [9], these parameters can be written as a sum of two terms:

$$B_p^k = B_{p,q}^k + B_{p,S}^k \tag{2}$$

The former contribution originates from the electrostatic interaction between valence electrons of an impurity ion and ions of crystal lattice, whereas the latter is proportional to the overlap of the wave functions of an impurity ion and ligands; it includes effects of the covalent bond formation and exchange interaction. Inclusion of these effects significantly improves agreement between the calculated and experimentally observed energy levels. Analytical expressions for calculating both contributions to the CFP in the case of 3*d*-ion are as follows [9]:

$$B_{p,q}^{k} = -K_{p}^{k} e^{2} \left\langle r^{p} \right\rangle \sum_{i} q_{i} \frac{V_{p}^{k}(\theta(i), \varphi(i))}{R(i)^{p+1}} \tag{3}$$

$$B_{p,S}^{k} = K_{p}^{k} e^{2} \frac{2(2p+1)}{5} \sum_{i} \left(G_{s} S_{s}(i)^{2} + G_{\sigma} S_{\sigma}(i)^{2} + \gamma_{p} G_{\pi} S_{\pi}(i)^{2} \right) \frac{V_{p}^{k}(\theta(i), \varphi(i))}{R(i)} \tag{4}$$

Eq. (3) describes the point charge contribution to the CFP, which appears due to electrostatic interaction between the central ion and the lattice ions enumerated by index *i* with charges q_i and spherical coordinates R_i, θ_i, φ_i (in the reference system centered at the impurity ion itself). The averaged values $\left\langle r^{p} \right\rangle$, where *r* is the radial coordinate of the *d* electrons of the impurity ion, can be obtained either from the literature or calculated numerically, using the radial parts of the corresponding ion's wave functions. The values of the numerical factors K_p^k, γ_p, the expressions for the polynomials V_p^k and the definitions of the operators O_p^k can all be found in Ref. [9]; for the sake of brevity, they are not given here. Eq. (4) determines the so called exchange charge contribution to the CFPs; it is proportional to the overlap between the wave functions of the central ion and ligands and thus includes all covalent effects. The $S(s), S(\sigma), S(\pi)$ entries correspond to the overlap integrals between the *d*-functions of the central ion and *p*- and *s*-functions of the ligands $S(s) = \langle d0 | s0 \rangle, S(\sigma) = \langle d0 | p0 \rangle, S(\pi) = \langle d1 | p1 \rangle$. The G_S, G_σ, G_π coefficients are dimensionless adjustable parameters of the model, whose values are determined from the positions of the first three absorption bands in the experimental spectrum. They can be approximated to a single value, i.e. $G_S = G_\sigma = G_\pi = G$, which then can be estimated from one absorption band only (the lowest in energy). This is usually a reasonable approximation [9]. The overlap integrals, which enter the above-given equations, correspond to the Fe^{6+}-O^{2-} wave functions overlaps, were calculated numerically, taking the wave functions from Ref. [11]. For a further convenience of use, they were approximated by the following exponential functions of the Fe^{6+}-O^{2-} distance *R* (expressed in a. u.) [17]:

$$\begin{aligned} S(s) &= \langle d0 | s0 \rangle = -0.71931 \ \exp(-0.88026 \ R) \\ S(\sigma) &= \langle d0 | p0 \rangle = 0.68957 \ \exp(-0.81694 \ R) \\ S(\pi) &= \langle d1 | p1 \rangle = 1.2686 \ \exp(-1.1485 \ R) \end{aligned} \tag{5}$$

The ECM has been successfully applied to numerous crystals doped with the transitional metal ions; more further details can be found in Refs. [17-22 and references therein].

CALCULATIONS OF THE CFPs

Using the crystal structure data from Refs. [13,14,16], we generated large clusters consisting of 15876 ions in K_2CrO_4, 27999 ions in K_2SO_4 and 37632 ions in K_2SeO_4, which include all ions of crystal lattice located at the distances up to 61.814 Å, 69.336 Å and 76.920 Å respectively, from the impurity ion. Such clusters are needed to achieve proper convergence of the crystal lattice sums, in ECM, especially those ones of the second rank, which depend on the distance R as $1/R^3$, and, as such, converge very slowly. Table 1 below collects the calculated values of CFPs for all considered systems. To illustrate the role and significance of the exchange charge contribution (ECC) in comparison with that one of the point charge contribution (PCC) both contributions to the total CFPs, are shown separately.

Table 1. CFPs (Stevens normalization) and Racah parameters B, C (all in cm^{-1}) for $K_2MO_4:Fe^{6+}$ (M= Cr, S, Se). G is the dimensionless ECM parameter.

CFPs	K_2CrO_4			K_2SO_4			K_2SeO_4		
	PCC	ECC	Total value	PCC	ECC	Total value	PCC	ECC	Total value
B_2^{-2}	42	74	116	206	333	539	-1309	-2939	-4248
B_2^{-1}	-	-	-	-	-	-	-1971	-7513	-9484
B_2^{0}	125	34	159	-25	-177	-202	-97	-745	-842
B_2^{1}	-	-	-	-	-	-	-1688	-5868	-7556
B_2^{2}	248	1077	1325	504	974	1478	-373	-1164	-1537
B_4^{-4}	795	7216	8011	-1241	-6051	-7292	1024	9922	10946
B_4^{-3}	-	-	-	-	-	-	1113	10573	11686
B_4^{-2}	1697	14934	16631	-2929	-13968	-16897	1324	12351	13675
B_4^{-1}	-	-	-	-	-	-	-654	-6457	-7111
B_4^{0}	86	790	876	150	731	881	46	463	509
B_4^{1}	-	-	-	-	-	-	853	8093	8946
B_4^{2}	-559	-5059	-5618	-875	-4238	-5113	-786	-7618	-8404
B_4^{3}	-	-	-	-	-	-	587	6060	6647
B_4^{4}	981	8959	9940	1778	8652	10430	660	6506	7166
G		18.393			9.961			19.752	
B		446.2			472.2			375	
C		1368.5			1278.3			1687.5	

It is seen that the ECC is, very often, greater than the PCC, which means the importance of the covalent effects against the point charge effect, in studied systems. It can be also noted that the ECM parameter *G* and the values of the exchange charge contribution to the CFPs (for the second rank CFPs especially) are considerably greater for K_2CrO_4 and K_2SeO_4.

Before we proceed with the energy level analysis, we consider and compare the crystal field invariants N_v in each of the three considered hosts. This quantity can be viewed as a reliable qualitative measure of the crystal field strength defined as [23, 24]

$$N_v = \left[\sum_{p,k} \left(B_p^k \right)^2 \frac{4\pi}{2p+1} \right]^{1/2} \tag{6}$$

where the CFPs values B_p^k, p=2,4 and k= -p,-p+1,….,p-1,p, are taken in the Wybourne normalization. Relations between the Stevens and Wybourne normalizations for the crystal field parameters can be found in Ref. [25].

The values of N_v, calculated with the CFPs parameters from Table 1 are colected in Table 2.

Table 2. Values of N_v (all in cm^{-1}) for $K_2MO_4:Fe^{6+}$ (*M*= Cr, S, Se).

N_v	K_2CrO_4	K_2SO_4	K_2SeO_4
N_v-*ECM*	31116.8	48841.6	33088.0

The direction of decreased crystal field invariants, calculated in actual site symmetry, give the trends of decreasing of the field strength of the doped crystals.

CALCULATIONS OF THE Fe^{6+} ENERGY LEVEL SCHEMES

The energy levels of the Fe^{6+} impurity ion doped in crystals K_2MO_4 (*M*=S, Cr, Se) are considered as the eigenvalues CF Hamiltonian:

$$H = H_0(B,C) + H_{CF}\left(B_p^k\right) \tag{7}$$

The sequence of the energy levels of the Fe^{6+} cation with its $3d^2$ electron shell, in the tetrahedral coordination, is determined mainly by the crystal field splitting of the ^3F and ^1D terms. The ground state is the $^3A_2$ (^3F), whereas the lowest excited states are the ^1E (^1D) and $^3T_2$(^3F) states. The relative positions of these spin-singlet and spin-triplet states are strongly affected by the local geometry around impurity. The low-symmetry crystal field effects, which arise from the deviation of the

$[FeO_4]^{2-}$ cluster, from the ideal T_d symmetry, would produce additional splitting of the orbital triplet states and shift the energy levels. One of the main characteristic features of the $K_2MO_4:Fe^{6+}$ spectra is the presence of the sharp ^1E-$^3A_2$ radiative transition; in addition, the excited state absorption spectra from ^1E state can gives more information about location of the higher excited states.

The low lying energy level schemes of the $K_2MO_4:Fe^{6+}$ systems were calculated by diagonalizing the crystal field Hamiltonian (7), with CFPs from Tables 1, in the basis spanned by 25 wave functions of all 5 terms of the $3d^2$ electronic configuration of free Fe^{6+} ion. The obtained, in this way, energy levels are collected in Tables 3 along with the experimental data [1, 4].

Table 3. Energy levels (in cm^{-1}) of $K_2MO_4:Fe^{6+}$ (M= Cr, S, Se).

Energy levels (T_d group not.)	K_2CrO_4			K_2SO_4			K_2SeO_4		
	Calculated this work	Averaged	Observed [1, 4]	Calculated this work	Averaged	Observed [1, 4]	Calculated this work	Averaged	Observed [1, 4]
$^3A_2$	0	0	0	0	0	0	0	0	0
^1E	6212 6215	6214	6214	6219 6231	6225	6225	6170 6278	6224	6224
$^1A_1$	11582	11582	9119	11678	11678	9176	11598	11598	9104
	13164			13135			11659		
$^3T_2$	13167	13280	13280	13301	13332	13330	12443	13000	≈13000
	13510			13560			14899		
	17739			17917			17203		
$^3T_1$	17862	17931	17930	18086	18200	18200	18175	18422	≈17700
	18191			18597			19887		
	19237			19215			17293		
$^1T_2$	19295	19405	-	19464	19465	-	18045	18658	-
	19684			19717			20636		
	21218			21260			21420		
$^1T_1$	21240	21396	-	21415	21579	-	22809	22877	-
	21729			22062			24403		
	28105			28215			25913		
$^3T_1$	28643	28638	-	29224	28916	-	28644	29111	-
	29165			29309			32776		
^1E	33025 33031	33028	-	33081 33144	33113	-	29856 31391	30624	-
	33456			33888			34037		
$^1T_2$	33892	33758	-	33930	33991	-	36670	36098	-
	33926			34155			37588		
$^1A_1$	42516	42516	-	42617	42617	-	45777	45777	-

In addition, Fig. 2a, 2b and 2c visualizes correspondence between the experimental spectra and calculated energy levels.

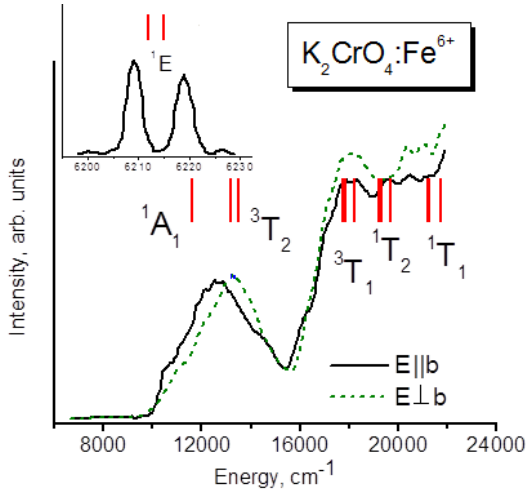

Fig. 2a. Experimental absorption spectra (solid lines) of $K_2CrO_4:Fe^{6+}$ and calculated Fe^{6+} energy levels (vertical lines) - adopted from [1].

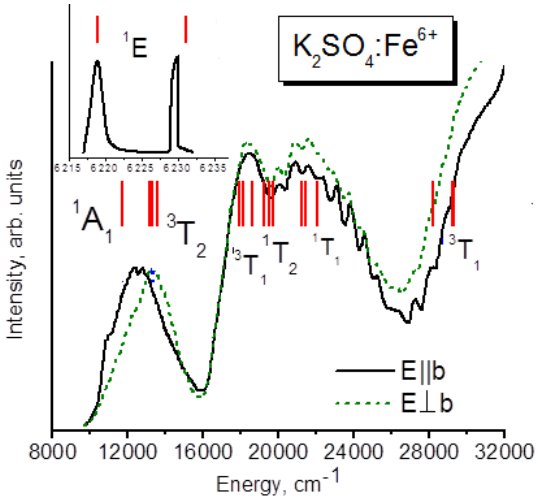

Fig. 2b. Experimental absorption spectra (solid lines) of $K_2SO_4:Fe^{6+}$ and calculated Fe^{6+} energy levels (vertical lines) - adopted from [4].

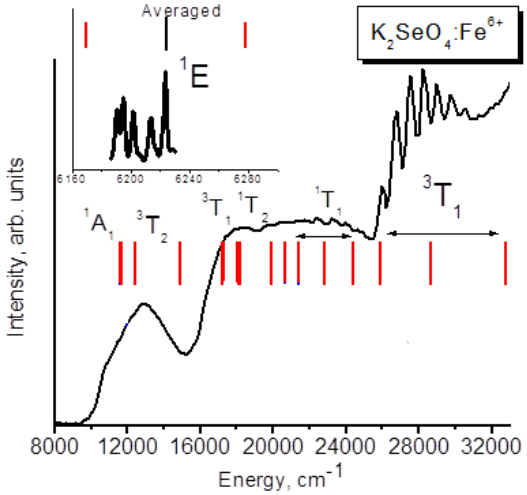

Fig. 2c. Experimental absorption spectra (solid lines) of $K_2SeO_4:Fe^{6+}$ and calculated Fe^{6+} energy levels (vertical lines) - adopted from [1].

All spectra are characterized by two prominent bands, which are due to the spin-allowed transitions $^3A_2 \rightarrow {}^3T_2(^3F)$ and $^3A_2 \rightarrow {}^3T_1(^3F)$, at about 13000 cm^{-1} and 18000 cm^{-1}, respectively. The latter one is mixed up with the spin-forbidden transitions to the $^1T_2$, $^1T_1$ states. A very weak absorption at about 6200 cm^{-1} is caused by the $^3A_2 \rightarrow {}^1E(^1D)$ transition.

We emphasize that application of the ECM with its calculations of all CFPs without any assumption about the impurity center symmetry allows for quantitative treatment of the low-symmetry crystal field effects, which is evidenced by the splitting of the orbital triplet and doublet states and complete removal of the degeneracy. The magnitude of this splitting is the largest in K_2SeO_4, where the splitting of the orbital triplets can be as large as ~7000 cm^{-1} for the $^3T_1(^3P)$ state (compare it with the splitting of just about 1000 cm^{-1} in the remaining two crystals).

When presenting the results, we give in the corresponding table the weighted averaged positions of all energy levels arising from the "parental" states of the T_d symmetry, which can be then directly compared to the experimental data from Ref. [1, 4]. On average, as is evidenced by Tables 3 and Fig. 2, agreement between these data is good. It can be noted that the calculated position of the $^1A_1$ state at about 11500 cm^{-1} is somewhat overestimated with respect to the experimental results [1, 4]; however, a similar overestimation was reported by the authors of Reference [4], after application of the angular overlap model.

Position of the $^3T_1(^3P)$ state at about 27000 - 28000 cm^{-1} is not shown in Fig. 2, since it is hidden by the strong charge transfer O^{2-} - Fe^{6+} transition.

As is known from the crystal field theory, the position of the $^3T_2(^3F)$ state of an ion with the d^2 configuration in the tetrahedral coordination determines the crystal field strength 10*Dq*. Collecting together the corresponding data for all considered crystals, we can arrange them in the order of the decreasing crystal strength as 10*Dq*(K_2SO_4)> 10*Dq*(K_2SeO_4)> 10*Dq*(K_2CrO_4), in full agreement with the direction of decreased crystal field invariants, calculated with the use of Eq. (6).

As it is well known [26], the Racah parameters *B* and *C* for transitional metal ions doped in different host matrices are significantly reduced with respect to those of free ion. To analyze this reduction, we introduce a non-dimensional quantity [27]

$$\beta = \sqrt{\left(\frac{B_1}{B_0}\right)^2 + \left(\frac{C_1}{C_0}\right)^2} \tag{8}$$

where subscripts "1" and "0" are related to the values of the Racah parameters in a host matrix and in a free state, respectively. This quantity can serve as a qualitative measure of the nephelauxetic effect in doped crystals. To calculate this parameter we need the values of the parameters B_0 and C_0 for free Fe^{6+} ion. These values B_0=1387 cm^{-1} and C_0=5292 cm^{-1} [28] have obtained by fitting the experimental values [29] of energy levels of free ferrate (VI) ion. With the relation (8), we obtained β = 0.412 for K_2CrO_4, β = 0.417 for K_2SO_4 and β = 0.418 for K_2SeO_4.Thus, the Fe^{6+}-O^{2-} bonds are more covalent in K_2CrO_4, less covalent in K_2SeO_4 with K_2SO_4 being between them.

CONCLUSIONS

In this paper we calculated the crystal field parameters for three K_2MO_4 crystals (*M*= Cr, S, Se) doped with Fe^{6+}. ECM of CF was used in the calculations, with takes into account the actual geometry of the impurity centers. With the obtained CFPs, the complete energy level scheme of the Fe^{6+} ions was calculated and comparison to the experimental absorption spectra yielded good agreement. The comparative analysis of the crystal field invariants and low symmetry crystal field effects (evidenced by the splitting of the orbital degenerated levels), was performed. The following trends were found: the crystal field strength decreases in the following sequence: $K_2SO_4 \rightarrow K_2SeO_4 \rightarrow K_2CrO_4$ (which agrees with the experimental absorption spectra), whereas the covalent effects are decreasing when going from K_2CrO_4 to less covalent in K_2SO_4 and, finally, K_2SeO_4. It was also demonstrated that proper description of the Fe^{6+} impurities in these crystals, including the CFPs, crystal field invariants, and splitting of the orbital degenerated states, requires knowledge and use of the actual symmetry of impurity centers.

ACKNOWLEDGMENT

M.G. Brik thanks the Programme for the Foreign Experts offered by Chongqing University of Posts and Telecommunications and the project PUT430 from Ministry of Education and Research of Estonia.

REFERENCES

1. T.C. Brunold, A. Hauser, H.U. Güdel, *J. Lumin*. 59, 321 (1994).
2. S. Kück, *Appl. Phys*. B72, 515 (2001).
3. L. Di Sipio, G. De Michelis, E. Baiocc, and G. Ingletto, *Transition Met. Chem*. 5, 164 (1980).
4. T.C. Brunold, H.U. Güdel, S. Kück and G. Hüber, *J. Lumin*. 65, 293 (1996).
5. D. Reinen, W. Rauw, U. Kesper, M. Atanasov, H.U. Gudel, M. Hazenkamp, U. Oetliker, *J. All. Comp*. 246, 193 (1997).
6. B. Wagner, D. Reinen, Th. C. Brunold and H.U. Gudel, *Inorg. Chem*. 34, 1934 (1995).
7. K. Wissing, M.T. Barriuso, J.A. Aramburu and M. Moreno, *J. Chem. Phys*. 111(22), 10217 (1999).
8. A. Al-Abdalla, L. Seijo and Z. Barandiaran, *J. Chem. Phys*. 109(15), 6396 (1999).
9. B.Z. Malkin, in A.A. Kaplyanskii, B.M. Macfarlane (Eds.), Spectroscopy of Solids Containing Rare-Earth Ions, North-Holland, Amsterdam, **1987**, p. 33.
10. C. Rudowicz, J. Qin*, J. Lumin*. 110, 39 (2004).
11. E. Clementi and C. Roetti, *Atomic Data and Nuclear Data Tables* 14, 177 (1974).
12. International Tables for Crystallography, Ed. T. Hahn, Vol. A, Springer Verlag, Berlin, **2006**, p. 298.
13. J.A. Mc Ginnety, *Acta Crystall*. B28, 2845 (1972).
14. K. Ojima, Y. Nishihata, A. Sawada, *Acta Crystall*. B51, 287 (1995).
15. R.W.G. Wyckoff, Crystal Structures, vol. 3, Interscience Publishers, Inc., New York, **1965**, p. 95.
16. N. Yamada, Y. Ono, and T. Ikeda, *J. Phys. Soc. Japan*, 53, 2565 (1984).
17. M.G. Brik, N.M. Avram and C.N. Avram Exchange charge model of crystal field for 3d ions, in: N.M. Avram and M.G. Brik (Eds), Optical Properties of 3d Ions in Crystals-Spectroscopy and Crystal Field Analysis, Tsinghua University Press, Springer, Beijing, Berlin, **2013**.
18. C. Jousseaume, D. Vivien, A. Kahn-Harari, B.Z. Malkin, *Opt. Mater*. 24, 143 (2003).
19. N.M. Avram, M.G. Brik, I.V. Kityk, *Opt. Mater.* 32**,** 1668 (2010).
20. M.G. Brik, C.N. Avram, *J. Lumin*. 131, 2642 (2011).
21. A.M. Srivastava, M.G. Brik, *J. Lumin.* 132, 579 (2012).
22. N. Mironova-Ulmane, M.G. Brik, I. Sildos, *J. Lumin.* 135**,** 74 (2013).
23. F. Auzel, O. Malta, *J. Phys.* 44**,** 201 (1983).
24. F. Auzel, *Opt. Mater.* 19, 89 (2002).
25. C. Rudowicz, *Mag. Res. Rev.* 13, 32 (1987).

26. B.N. Figgis, M.A. Hitchman, Ligand field theory and its application, Wiley-VCH, New York, **2000**, p 218.
27. M.G. Brik, N.M. Avram, C. N. Avram, *Physica* B371, 43 (2006).
28. E.-L. Andreici, A.S. Gruia, N.M. Avram, *Phys. Scr.* T149**,** 014060 (2012).
29. Yu Ralcenko, A.E. Kramida, J. Reader and NIST ASD Team (2011), *NIST Atomic Spectra Database* (ver. 5. 0), National Institute of Standards and Technology, Gaithersburg, MD, *http://physics.nist.gov/cgi-bin/ASD/energy1.pl*